Rigid Rod Molecules as Liquid Crystal Thermosets. II. Rigid Rod Esters

ANDREA E. HOYT and BRIAN C. BENICEWICZ,* *Materials Science and Technology Division, Los Alamos National Laboratory, Los Alamos, New Mexico 87545*

Synopsis

Nine rigid rod ester monomers endcapped with maleimide, nadimide, and methylnadimide groups were prepared and studied by DSC and hot stage polarized light microscopy. All of the monomers showed thermotropic nematic liquid crystalline phases and could be thermally crosslinked in the nematic phase. The nematic texture was maintained in the crosslinked solid state. The nematic phase range was enlarged by B-staging the monomeric compounds. Heating the monomers for a short period of time in the nematic phase lowered the crystal to nematic transition temperatures and increased the nematic to isotropic transition temperatures. A nonequilibrium phase diagram was proposed to explain the melting behavior of these reactive liquid crystal thermoset materials.

INTRODUCTION

Part I of this series addressed a group of rigid rodlike amide molecules designed to test the feasibility of making liquid crystalline thermoset (LCT) materials that could be crosslinked in the liquid crystalline phase with retention of the order in the final crosslinked solid. Although thermotropic nematic phases were obtained for three examples, the crystal to nematic melting transitions could only be observed at very high heating rates. The high heating rates were necessary to preclude significant crosslinking in the solid state during heating of the sample. The nematic phase region was generally narrow (approximately 5°C) and crosslinking occured quite fast at the high melting temperatures of these monomers. For melt processing, this limited range nematic behavior would be too restrictive for many applications.

It is well known in the study of low molecular mass liquid crystals that molecules based on aromatic amide containing mesogens are high melting, often to such an extent that mesomorphic behavior is not observed. Although some thermotropic liquid crystalline aromatic amides have been synthesized, there are far fewer examples than thermotropic liquid crystalline aromatic esters.[1-4] The comparitively lower melting temperatures of the liquid crystalline esters are presumably due to the lack of strong intermolecular hydrogen bonds.

In an effort to reduce the melting points of liquid crystal thermoset monomers, a series of ester based monomers were prepared and studied. In this paper, results are presented and discussed for ester based monomers designed according to the liquid crystal thermoset concept.

* To whom correspondence should be addressed.

Journal of Polymer Science: Part A: Polymer Chemistry, Vol. 28, 3417–3427 (1990)

Published by John Wiley & Sons, Inc. CCC 0887-624X/90/123417-11$04.00

EXPERIMENTAL

Characterization

Differential scanning calorimetry (DSC) was performed with a Perkin-Elmer DSC-2C at a heating rate of 20°C min^{-1} under an argon atmosphere unless noted otherwise. Microscopy was performed with a Bausch and Lomb Micro-Zoom™ Microscope equipped with crossed polarizers and a Kofler hot stage controlled by a variable transformer. Infrared (IR) spectra were recorded on a Perkin-Elmer 283 Spectrophotometer using KBr pellets. Proton (^1H) nuclear magnetic resonance (NMR) spectra were recorded using a JEOL PMX60SI Spectrometer at 60 MHz. Chemical shifts are reported in parts per million downfield from tetramethylsilane.

Materials and Monomer Synthesis

Hydroquinone, methylhydroquinone, and chlorohydroquinone were purchased from Aldrich. The chlorohydroquinone was recrystallized from chloroform, toluene, and then washed in a Soxhlet extractor with hexane for 6 h before use. All other reagents were used without further purification. The general method used to prepare the monomers is shown in Figure 1. The endgroups were synthesized by reacting *p*-aminobenzoic acid with the appropriate anhydride,[5] cyclodehydrating with acetic anhydride and sodium acetate,[6] and finally converting to the acid chloride by treatment with oxalyl chloride.[7] The detailed procedures can be found in Part I. In general, the monomers were prepared by dissolving or suspending one equivalent of the diol in diethyl ether or chloroform with two equivalents of triethylamine. The solution or suspension was chilled in an ice bath and 2 equiv. of the acid chloride were carefully added with good stirring. In some cases an exotherm was noted upon addition of the acid chloride. The reaction mixture was stirred for 30 min. The product was

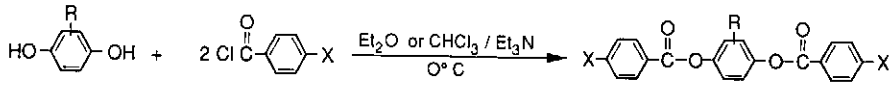

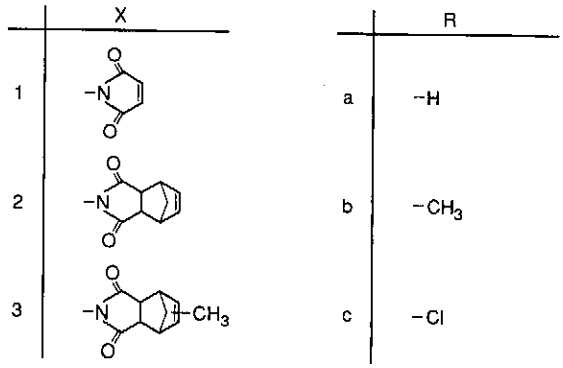

Fig. 1. Reaction scheme for the synthesis of rigid rod ester monomers.

then precipitated in hexane if necessary and collected by suction filtration. Recrystallization from an appropriate solvent was followed by drying under vacuum at 80°C.

*Hydroquinone Bismaleimide Ester (**1a**)*

This compound was recrystallized from 60/40 (v/v) phenol/tetrachloroethane.

IR, cm^{-1}: 3130–3080 (w) (arom. C—H), 1735 (s) (ester C=O), 1715 (s) (imide C=O). ^{1}H-NMR (CF_3COOD): δ 8.1 (dd, 8H, J_1 = 40 Hz, J_2 = 8 Hz), 7.4 (s, 4H), 7.1 (s, 4H).

ANAL. Calcd for $C_{28}H_{16}N_2O_8$: C, 66.05; H, 3.27; N, 5.42. Found: C, 66.15; H, 3.17; N, 5.51.

*Hydroquinone Bisnadimide Ester (**2a**)*

This compound was recrystallized from tetrachloroethane/hexane.

IR, cm^{-1}: 3200–3000 (w) (arom., aliph. C—H), 1735 (s) (ester C=O), 1710 (s) (imide C=O). ^{1}H-NMR (CF_3COOD): δ 8.6–7.0 (12H), 6.4 (s, 4H), 3.7 (8H), 1.9 (dd, 4H, J_1 = 4 Hz, J_2 = 10 Hz).

ANAL. Calcd for $C_{34}H_{28}N_2O_8$: C, 68.47; H, 4.14; N, 4.10. Found: C, 67.21; H, 4.76; N, 4.73.

*Hydroquinone Bis(methylnadimide) Ester (**3a**)*

This compound was purified by extraction with hexane.

IR, cm^{-1}: 3100 (w) (arom. C—H), 2980 (w) (aliph. C—H), 1740 (s) (ester C=O), 1715 (s) (imide C=O). ^{1}H-NMR (CF_3COOD): δ 8.1 (dd, 8H, J_1 = 38 Hz, J_2 = 8 Hz), 7.5 (s, 4H), 6.1 (s, 2H), 3.0–3.9 (t, 8H), 2.0 (s, 6H), 1.8 (s, 4H).

ANAL. Calcd for $C_{36}H_{32}N_2O_8$: C, 71.17; H, 4.66; N, 4.08. Found: C, 69.67; H, 5.20; N, 4.51.

*Methylhydroquinone Bismaleimide Ester (**1b**)*

This compound was recrystallized from 1,2-dichloroethane/hexane.

IR, cm^{-1}: 3110 (w) (arom. C—H), 3080 (w) (aliph. C—H), 1735 (s) (ester C=O), 1715 (s) (imide C=O). ^{1}H-NMR ($CDCl_3$): δ 8.0 (dd, 8H, J_1 = 36 Hz, J_2 = 8 Hz), 7.2 (d, 3H, J = 4 Hz), 6.9 (s, 4H), 2.3 (s, 3H).

ANAL. Calcd for $C_{29}H_{18}N_2O_8$: C, 66.74; H, 3.50; N, 5.32. Found: C, 66.67; H, 3.47; N, 5.36.

*Methylhydroquinone Bisnadimide Ester (**2b**)*

This compound was recrystallized from 1,2-dichloroethane/hexane.

IR, cm^{-1}: 3080 (w) (arom. C—H), 2990 (w) (aliph. C—H), 1730 (s) (ester C=O), 1705 (s) (imide C=O). ^{1}H-NMR ($CDCl_3$): δ 8.25 (dd, 8H, J_1 = 48 Hz, J_2 = 6 Hz), 7.15 (s, 3H), 6.3 (s, 4H), 3.5 (s, 8H), 2.25 (s, 3H), 1.7 (s, 4H).

ANAL. Calcd for $C_{39}H_{30}N_2O_8$: C, 69.34; H, 4.68; N, 4.04. Found: C, 71.55; H, 4.62; N, 4.28.

*Methylhydroquinone Bis(methylnadimide) Ester (**3b**)*

This compound was recrystallized from toluene/hexane.

IR, cm^{-1}: 3100 (w) (arom. C—H), 2980 (w) (aliph. C—H), 1740 (s) (ester C=O), 1725 (s) (imide C=O). ^{1}H-NMR ($CDCl_3$): δ 7.85 (dd, 8H, J_1 = 42

Hz, J_2 = 8 Hz), 7.2 (s, 3H), 5.9 (s, 2H), 3.3, 3.2, 2.9 (s, 8H), 1.9 (s, 6H), 1.6 (s, 4H).

ANAL. Calcd for $C_{41}H_{34}N_2O_8$: C, 70.32; H, 5.18; N, 4.20. Found: C, 72.13; H, 5.02; N, 4.10.

*Chlorohydroquinone Bismaleimide Ester (**1c**)*

This compound was recrystallized from methylene chloride/hexane.

IR, cm^{-1}: 3100 (w) (arom. C—H), 1745 (s) (ester C=O), 1725, 1715 (s) (imide C=O). ^{1}H-NMR ($CDCl_3$): δ 8.1 (dd, 8H, J_1 = 24 Hz, J_2 = 2 Hz), 8.1 (s, 3H), 7.3 (s, 4H).

ANAL. Calcd for $C_{28}H_{15}ClN_2O_8$: C, 62.03; H, 3.03; Cl, 6.38; N, 4.90. Found: C, 61.95; H, 2.79; Cl, 6.53; N, 5.16.

*Chlorohydroquinone Bisnadimide Ester (**2c**)*

This compound was recrystallized from 1,1,2-trichloroethane/hexane.

IR, cm^{-1}: 3080 (w) (arom. C—H), 2990 (w) (aliph. C—H), 1738 (s) (ester C=O), 1710 (s) (imide C=O). ^{1}H NMR (CF_3COOD): δ 8.5 (dd, 3H, J_1 = 6 Hz, J_2 = 2 Hz), 6.5 (d, 8H, J = 8 Hz), 6.5 (s, 4H), 3.9, 3.8, 3.7 (s, 8H), 2.95 (dd, 4H, J_1 = 6 Hz, J_2 = 8 Hz).

ANAL. Calcd for $C_{38}H_{27}ClN_2O_8$: C, 65.14; H, 3.79; Cl, 7.52; N, 3.89. Found: C, 67.61; H, 4.03; Cl, 5.25; N, 4.15.

*Chlorohydroquinone Bis(methylnadimide) Ester (**3c**)*

This compound was recrystallized from acetone/water.

IR, cm^{-1}: 3080 (w) (arom. C—H), 2980 (w) (aliph. C—H), 1745 (s) (ester C=O), 1710, 1705 (s) (imide C=O). ^{1}H-NMR (CF_3COOD): δ 8.4 (dd, 3H, J_1 = 5 Hz, J_2 = 3 Hz), 7.75, 7.5, 7.35 (s, 8H), 6.0 (s, 2H), 3.45, 3.3, 3.0 (s, 8H), 2.0 (d, 6H, J = 2 Hz), 1.7 (s, 4H).

ANAL. Calcd for $C_{40}H_{31}ClN_2O_8$: C, 68.23; H, 4.45; Cl, 5.27; N, 3.94. Found: C, 68.33; H, 4.38; Cl, 5.04; N, 3.98.

RESULTS AND DISCUSSION

Synthesis

The synthesis of the ester monomers discussed in this paper was very similar to that of the amide monomers synthesized in Part I of this series. The central units for the esters were based on substituted and unsubstituted hydroquinones. It is well known that lateral substituents on low molecular mass liquid crystals generally lower the melting transitions relative to their unsubstituted analogues but also often decrease the mesomorphic thermal stability of both smectic and nematic phases.[8] There are several methods that have been used to lower the transition temperatures of thermotropic polyesters without decreasing the aromatic nature or the rodlike character of the polymer. One method that has been explored quite successfully is based on monomers that contain a parallel but offset bonding geometry. This crankshaft geometry is probably best illustrated by the thermotropic polyesters derived from the 2,6-functionally disubstituted naphthalene monomers and various other para-linked monomers.[9] Another method that was successful in lowering the transition temperatures of

wholly aromatic polyesters was the polymerization or copolymerization of para-substituted monomers containing lateral substituents.[10,11] It is this latter method of lowering transition temperatures that we have applied to the design and preparation of melt processable LCT's. Other modifications of aromatic polyesters have been explored to reduce melting transitions such as the use of bent rigid units found in monomers with meta linkages and monomers containing molecular swivels.[12] However, these monomers usually adversely affect the properties of the polymers and only limited amounts of these monomers can be incorporated into the polymer before the liquid crystalline nature of the material is lost.

The monomers were synthesized according to the general scheme shown in Figure 1 using a Schotten–Baumann type procedure as described in Part I.

Thermal Behavior

All of the monomers were analyzed by differential scanning calorimetry (DSC) and hot stage polarized light microscopy. The DSC traces were quite difficult to interpret, particularly for the bisnadimide and bismethylnadimide monomers. This is likely due to the large number of processes that can occur, sometimes simultaneously, such as melting, addition reactions leading to crosslinking, reverse Diels–Alder reactions and subsequent crosslinking reactions of the newly formed species, gas evolution of some of the reverse Diels-Alder products, and isotropization. Optical microscopy was very useful in elucidating the behavior of these new materials and most of the discussion in this paper will focus on these observations. The microscope observations during heating and cooling were performed at various heating rates between 10 and 50°C min^{-1}, depending to a great extent on the nature of the sample. The temperatures reported are not equilibrium transition temperatures. Barrall and Sweeney[13] have reported that the major change in anisotropy as observed by optical microscopy does not always coincide with the maximum heat consumption as determined by DSC. It must be noted that these monomers are reactive systems and sometimes fast heating rates were needed to define the general behavior of the monomer before substantial reaction occurred.

The transition temperatures as determined by optical microscopy are shown in Tables I–III. The transitions of the chlorohydroquinone based monomers were not as clearly defined as those for the other monomers. Analysis of the purified chlorohydroquinone starting material by GC/MS showed small amounts (2–5%) of unsubstituted hydroquinone and dichlorohydroquinone present. It is suspected that the transition temperatures observed may have been depressed and/or broadened due to the mixture of monomers in this preparation. All of the monomers investigated in this study showed crystal to nematic melting transitions upon heating. For the bismaleimides in Table I, the crystal to nematic transition temperatures ranged from 215 to 282°C. A fluid nematic phase was observed for all of these monomers. At higher temperatures, the bismaleimides crosslinked before isotropization was observed, even at the highest heating rates. The nematic texture was retained upon solidification and was not affected by forceful attempts to shear the cover slide. The samples were cooled to room temperature and, after several days, there were no detectable changes in the nematic texture. The solidification temper-

TABLE I
Thermal Behavior of Bismaleimides

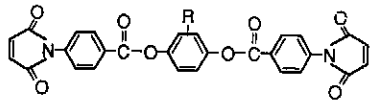

Monomer	R	Transitions[a] (°C)	
		$k \rightarrow n$	Solidification
1a	—H	282	293
1b	—CH_3	245	280
1c	—Cl	215	270

[a] Transition temperatures determined by polarized light microscopy, heating rate approximately 20°C min^{-1}.

atures in Table I are based on observations for a particular heating rate (approximately 20°C min^{-1}). The crosslinking and solidification of these materials were both time and temperature dependent. Slower heating rates resulted in the observation of a lower solidification temperature. The DSC curves for the bismaleimides were characterized by a sharp melting endotherm followed closely by a crosslinking exotherm. The peak exotherm temperatures were approximately 290°C for these monomers. A representative DSC curve is shown in Figure 2. When **1c** was heated isothermally in the nematic phase at 225°C, a fluid nematic phase was present for about 15 min, after which the birefringent sample had solidified and could not be sheared by the cover slide. For comparison, the amide monomers reported in the previous paper usually solidified within seconds after melting. The increase in time before solidification was most likely due to the lower melting temperature of the ester and consequently the slower reaction times.

The transitions of the bisnadimides are given in Table II. The crystal to nematic transition temperatures for the bisnadimides were higher than the

TABLE II
Thermal Behavior of Bisnadimides

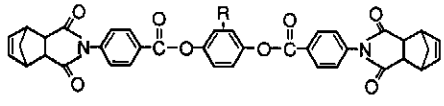

Monomer	R	Transitions[a] (°C)		
		$k \rightarrow n$	$n \rightarrow i$	Solidification
2a	—H	307	—	328
2b	—CH_3	271	286	—
2c	—Cl	271	310	—

[a] See Table I.

TABLE III
Thermal Behavior of Bis(methylnadimide)s

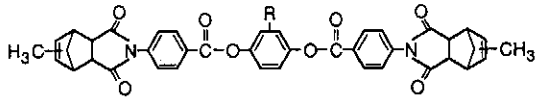

Monomer	R	Transitions[a] (°C) $k \rightarrow n$	$n \rightarrow i$
3a	—H	288	311
3b	—CH_3	211	259
3c	—Cl	255	274

[a] See Table I.

analogous bismaleimides. However, clearing points were observed for the substituted bisnadimides (**2b, 2c**) when viewed at normal heating rates, i.e., approximately 20°C min^{-1}. These were the first materials that showed both melting and clearing points at normal heating rates. The unsubstituted bisnadimide, **2a,** melted into a nematic phase at 307°C but solidified, presumably due to crosslinking, at 328°C upon continued heating. An isotropic phase for **2a** was observed, but only when a sample was placed onto a preheated 350°C hot stage. All of the bisnadimides showed some gas evolution and bubble formation after melting into the nematic phase. The mechanisms postulated for the curing of nadimide resins involve reverse Diels–Alder reactions and the formation of

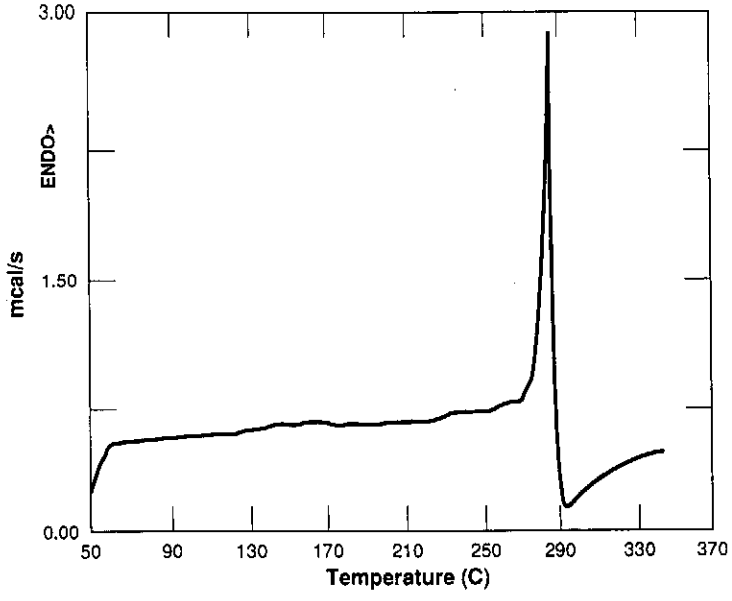

Fig. 2. DSC curve of bismaleimide, **1a**; heating rate 20°C min^{-1}.

cyclopentadiene. The release of some of the cyclopentadiene would cause bubble formation. We have also inferred the occurrence of these reactions from the distinctive odor that is detected concurrently with bubble formation.

The bismaleimides and bisnadimides could be supercooled after melting into the nematic phase. The nematic texture and fluid flow were retained below the original crystal to nematic transition temperature of the monomer. Also, the nematic texture was usually maintained after solidification. If the samples were cooled prior to extensive reaction and crosslinking, a second heating of these materials displayed a depression in the crystal to nematic transition temperature that could be greater than 50°C. It is proposed here that the melting point depression arose from the large number of new molecular species that were created during the initial stages of reaction. As mentioned in Part I, there has been considerable discussion concerning the curing of nadimide resins. There is general agreement that reverse Diels–Alder reactions occur during the curing of these resins and a large number of possible Diels–Alder adducts could be formed at the early stages of reaction. Some of the structures that could be formed are shown in Figure 3. Several studies have produced evidence for the formation of at least some of the proposed structures.[14–16] It is the multiplicity of products at the early stages of reaction that led to the large depression in melting points observed for these systems.

As reported earlier, the bisnadimides were the first materials for which the isotropic phase was detected at normal heating rates. An interesting phenomenon was observed during the isothermal heating of the samples in the isotropic phase that was common for all the bisnadimides. When **2b** was heated to 300°C

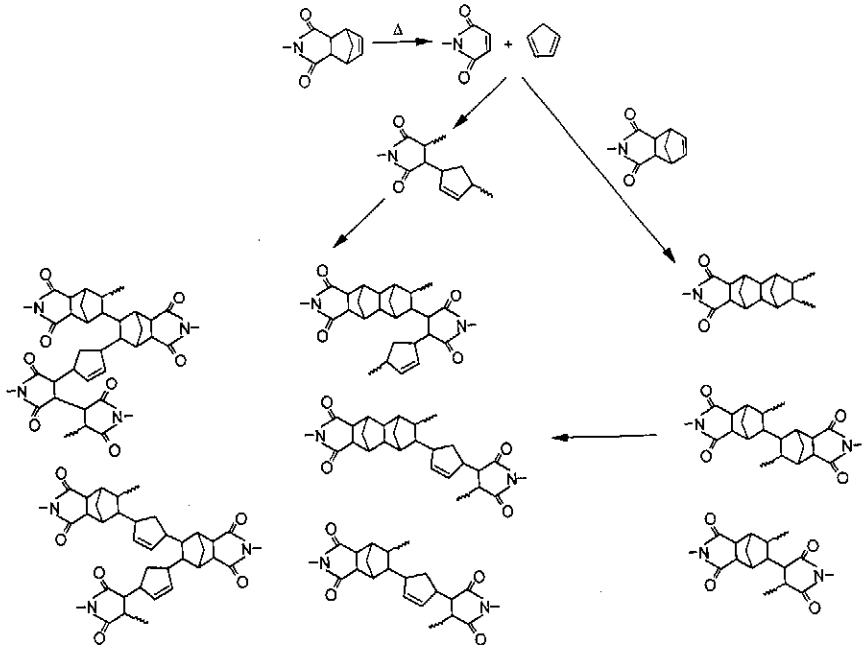

Fig. 3. Possible structures formed during the curing of nadimide terminated monomers, adapted from References 14–16.

and held isothermally, the monomer melted into the isotropic phase as indicated in Table II. However, after approximately 5 min nematic droplets were observed to form within the isotropic fluid. During the next 15 min the nematic droplets increased in number, coalesced, and eventually formed a continuous and complete nematic phase that could be sheared by the cover slip. After an additional 5 min, the material had solidified and could not be sheared. The reappearance of the nematic phase can be explained in terms of a reactive system. At the melting or isotropization temperatures of the monomer the reactions shown in Figure 3 occur readily leading to a mixture of products and *chain extension.* The oligomers produced at the early stages of reaction have a higher length to diameter ratio and probably a higher isotropization temperature than the original monomer. When a sufficient fraction of higher molecular weight species was produced at constant temperature, phase separation occurred and nematic droplets were observed. A continuous nematic phase was observed as the length and concentration of oligomers increased with time. This material eventually solidified in the nematic phase when the extent of reaction (both chain extension and crosslinking) reached higher values. The behavior of the materials can be schematically represented by the graph in Figure 4. Thus, the combination of chain extension and the formation of multiple oligomeric products leads to a broadening or enhancement of the nematic phase region. However, as chain extension and crosslinking proceed to advanced stages both the melting point and clearing point increase, eventually leading to solidification of the partially crosslinked solid with nematic type order. The diagram in Figure 4 is consistent with the observations made by hot stage microscopy.

The thermal data for the bis(methylnadimide)s are shown in Table III. All of these monomers displayed crystal to nematic and nematic to isotropic transitions. The thermal stability range of the nematic phase on first heating was as large as 48°C for **3b.** However, as discussed previously, the nematic phase range was enlarged by heating for a short period of time in the nematic phase. For example, **3c** was heated for a short time at 270°C and cooled to room temperature. On second heating, the sample melted into a fluid nematic phase

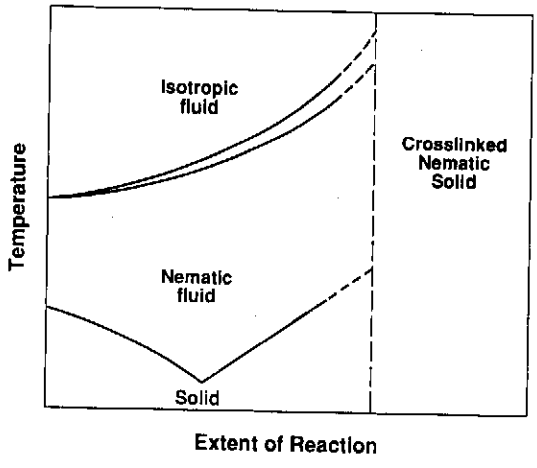

Fig. 4. Schematic phase diagram for the general melting behavior of LCT's.

at 185°C. This corresponded to a 70°C decrease in the crystal to nematic transition temperature compared with the first heating of the original monomer. The general behavior of the bis(methylnadimide)s was also represented by the schematic phase diagram in Figure 4, although the bis(methylnadimide)s appeared to be slower reacting than the bisnadimides. Monomer **3c** was heated on the microscope to 282°C and held isothermally. At this temperature the monomer was initially in the isotropic phase. The appearance of nematic droplets in the isotropic fluid was noticed after 10 min. The fluid was completely nematic after 60 min. Solidification in the nematic phase occurred approximately 120 min after the sample was melted.

Solubility

Solubilities of the monomers were tested in methylene chloride, chloroform, 1,1,2,2-tetrachloroethane (TCE), trifluoroacetic acid, 60/40 phenol/TCE, acetone, and ethyl acetate. None of the monomers showed high solubility and the maximum achieved was 15% (w/w) for **3c** in 1,1,2,2-tetrachloroethane. Solubilities of the other compounds were generally less than 10% (w/w) in all solvents tested. It should be noted, however, that the solubilities of the substituted hydroquinone monomers were higher than those of the unsubstituted hydroquinone monomers. Also, the solubilities of the chloro-substituted monomers (**1c, 2c, 3c**) were higher than those of the methyl-substituted monomers (**1b, 2b, 3b**).

CONCLUSION

Three series of ester based rigid rod monomers were prepared and studied by DSC and hot stage polarized light microscopy. These difunctional rigid rod monomers were endcapped with maleimide, nadimide, and methylnadimide groups. All of the monomers showed crystal to nematic transitions and were easily polymerized in the nematic phase. In addition, the bisnadimides and bis(methylnadimide)s exhibited nematic to isotropic transitions. The maleimide terminated monomers appeared to react the fastest of the three series and crosslinked in the nematic phase at normal heating rates. The methylnadimide terminated monomers reacted the slowest of the three series and could be observed in the fluid nematic state for up to two hours before solidification of the sample. With one exception, the melting points were below 300°C. The melting transitions could be substantially lowered by heating for a short time in the nematic phase. This B-staging period also influenced the nematic to isotropic transitions. It was proposed that chain extension, which occurred during the reactions leading to crosslinking, led to an increase in clearing point temperatures. The effect of chain length on the clearing points of liquid crystal polymers has been studied and our proposal is in agreement with these studies.[17,18] Based on the data presented here, a general nonequilibrium phase diagram was proposed to explain the behavior of the LCT monomers. Further work will determine the general applicability of the proposed diagram.

The solubilities of the monomers were low and probably not sufficient for processing of these monomers from solution. However, the melting points of the monomers and B-staged materials investigated in this study indicate that melt processing of such materials could be a viable route to new LCT matrix composites.

We are indebted to Sandra Cisneros–Flores for her assistance with the thermal analysis and to Robert Hermes for his assistance with GC/MS and helpful comments on the manuscript. The Materials Science and Technology Division and the Center for Materials Science of Los Alamos National Laboratory are gratefully acknowledged for support of this work. We also thank Professor S. J. Huang of the University of Connecticut for many helpful discussions.

References

1. E.-W. Choe and R. Mininni, *Mol. Cryst. Liq. Cryst.*, **49**, 133 (1979).
2. R. A. Vora and R. Gupta, *Mol. Cryst. Liq. Cryst.*, **67**, 215 (1981).
3. A. C. Griffin, T. R. Britt, G. A. Campbell, *Mol. Cryst. Liq. Cryst. Lett.*, **82**, 145 (1982).
4. V. Kalyvas and J. E. McIntyre, *Mol. Cryst. Liq. Cryst.*, **80**, 105 (1982).
5. F. Bergmann and D. Schapiro, *J. Org. Chem.*, **7**, 419 (1982).
6. B. S. Rao, *J. Polym. Sci. Polym. Lett. Ed.*, **26**, 3 (1988).
7. R. Adams and L. Ulich, *J. Am. Chem. Soc.*, **42**, 599 (1920).
8. G. W. Gray, *Molecular Structure and the Properties of Liquid Crystals*, Academic, New York, 1962, chapter 10.
9. G. W. Calundann, in *High Performance Polymers: Their Origin and Development;* R. B. Seymour and G. S. Kirshenbaum, Eds., Elsevier, New York, 1986, pp. 235–249.
10. W. J. Jackson, Jr., *Contemp. Top. Polym. Sci.*, **5**, 177 (1984).
11. R. Sinta, R. A. Minns, R. A. Gaudiana, and H. G. Rogers, *J. Polym. Sci. Polym. Lett. Ed.*, **25**, 11 (1987).
12. W. J. Jackson, Jr., *Br. Polym. J.*, **12**, 154 (1980).
13. E. M. Barrall, II and M. A. Sweeney, *Mol. Cryst. Liq. Cryst.*, **5**, 257 (1969).
14. R. W. Lauver, *J. Polym. Sci. Polym. Chem. Ed.*, **17**, 2529 (1979).
15. A. C. Wong, W. H. Ritchey, *Macromolecules*, **14**, 825 (1981); A. C. Wong, A. N. Garroway, and W. H. Ritchey, *Macromolecules*, **14**, 832 (1981).
16. J. N. Hay, J. D. Boyle, S. F. Parker, and D. Wilson, *Polymer*, **30**, 1032 (1989).
17. R. B. Blumstein and E. Stickles, *Proc. 28th IUPAC Macromol. Symp.*, 799 (1982).
18. R. B. Blumstein, E. M. Stickles, M. M. Gauthier, A. Blumstein, and F. Volino, *Macromolecules*, **17**, 177 (1984).

Received January 16, 1990
Accepted April 17, 1990